



Passivation effect of tunnel oxide grown by N₂O plasma for c-Si solar cell applications



Minhan Jeon ^a, Jiyeon Kang ^a, Gyeongbae Shim ^a, Shihyun Ahn ^a, Nagarajan Balaji ^b,
Cheolmin Park ^b, Youn-Jung Lee ^a, Junsin Yi ^{a,*}

^a College of Information and Communication Engineering, Sungkyunkwan University, Suwon, Republic of Korea

^b Department of Energy Science, Sungkyunkwan University, Suwon, Republic of Korea

ARTICLE INFO

Article history:

Received 25 January 2017

Received in revised form

21 March 2017

Accepted 24 March 2017

Available online 31 March 2017

Keywords:

Silicon oxide

Plasma oxidation

Passivation

N₂O

Carrier-selectivity

ABSTRACT

Electron-hole pair (EHP) recombination is a decreasing factor of the efficiency in silicon solar cells. The passivation layer reduces recombination by removing dangling bonds which act as recombination centers. Usually, SiN_x, SiO_x, SiON_x and AlO_x layers are used as passivation layer in solar cell applications. Tunnel oxide layer is one of the main issues to achieve high-quality passivation using carrier-selectivity between the silicon wafer and poly-Si layer. In this work, ultra-thin tunnel oxide layer by plasma enhanced chemical vapor deposition using N₂O plasma is deposited on both sides of the samples. The RF power and substrate temperature are varied. Then phosphorus doped Si layer is deposited. The optimized tunnel oxide layer has low D_{it} ($5.3 \times 10^{10} \text{ cm}^{-2} \text{ eV}^{-1}$) and high passivation effect (τ_{eff} of 923 μs , V_{oc} of 739 mV) when deposited with RF power of 200 W and a substrate temperature of 400 °C. This optimized tunnel oxide passivation layer is applied to the n-type c-Si solar cell. The fabricated solar cell showed J_{sc} of 41.04 mA/cm² and V_{oc} of 644 mV. Compared to the cell with chemical oxide passivation, J_{sc} and V_{oc} increased by 0.2 mA/cm² and 11 mV which were also higher than the cell with SiN_x passivation.

© 2017 Elsevier Ltd. All rights reserved.

1. Introduction

In order to reduce the silicon cost of solar cells, thinning of wafers has been tried [1]. It is predicted that the thickness of a wafer will decrease to about 100 μm by 2026 [2]. To increase the cost effectiveness of reducing wafer thickness and manufacturing costs, the main issue in solar cell research is to develop high efficient solar cells with a simple process and manufacturing through new technology developments. To fabricate high-efficiency solar cells, the lifetime of the minority carriers must be improved by minimizing the electrical loss of the photo-generated carriers and minimizing the optical loss of the light incident on the solar cells through anti-reflection coating (ARC). Since the research on the optical loss of the crystalline silicon surface [3] has been carried out to some extent, the research on the electrical loss would be more meaningful. In addition, to compensate the reduced short

circuit current when the wafer gets thinner, the surface recombination rate, electrical loss, and optical loss should be reduced [4,5]. The surface passivation becomes more important as the silicon wafer becomes thinner because the surface recombination velocity (SRV) is further reduced as the wafer thickness (W) decreases as shown in equation (1), thereby achieving a high effective lifetime.

$$\frac{1}{\tau_{\text{eff}}} = \frac{1}{\tau_{\text{bulk}}} + \frac{SRV_{\text{front}} + SRV_{\text{rear}}}{W} \quad (1)$$

where τ_{eff} is the effective lifetime, τ_{bulk} is the bulk lifetime.

In order to reduce the surface recombination, the surface passivation must be well performed so that the photo-generated carriers are collected on the electrode without recombination.

Recently, the researchers focus on carrier selective contacts to achieve the higher conversion efficiencies close to the theoretical limit of 29.4%. The vital element of this contact is the tunnel oxide is its outstanding interface passivation and reduces the minority carrier recombination as well as does not restrain the majority

* Corresponding author. 300 Cheoncheon-dong, Jangan-gu, Suwon 440-749, Republic of Korea.

E-mail address: junsin@skku.edu (J. Yi).

carrier flow at the rear metal contact. This is partially ascribed to the barrier height variation and effective mass in the oxide which precept the tunneling probability [6]. The tunnel oxide has been grown by various means such as wet chemical HNO_3 [7], dry grown UV/O_3 oxide [8] and a wet chemical oxide grown in ozonized $\text{DI-H}_2\text{O DIO}_3$.

Feldmann et al. [7] have demonstrated TOPCon cells with the tunnel oxide layer grown in 68 wt% nitric acid at a temperature of 110°C , close to its boiling point of 120°C [9,10]. However, the uniformity of the oxide and this wet chemical oxide is not industrially suitable. Moldovan et al. grown the tunnel oxide layer using ozone (DIO_3) and UV/O_3 and compared their results with the wet chemical HNO_3 oxide. UV/O_3 tunnel oxide cannot achieve the full implied voltage potential due to the stoichiometry of the interfacial layer and hence reduction in the efficiency [8]. Though the tunnel oxides grown by various methods were used for high efficiency silicon solar cells, very scarce report is available for the plasma grown tunnel oxide grown. Hence in this manuscript, the passivation effect of the plasma grown tunnel oxide has been studied for the fabrication of high efficiency solar cells.

2. Experiments

Fig. 1 represents the schematic of the solar cell used for this study. The solar cells were made from n-type mono-crystalline Czochralski (Cz) wafer with (100) orientation, $200\ \mu\text{m}$ thickness and $1\text{--}3\ \Omega\text{-cm}$ resistivity. Saw damage was removed in 8% NaOH before texturing. Texturing was then conducted with 2% NaOH to form random pyramids. The front boron diffused emitter was formed by Boron Tribromide (BBr_3) doping in a diffusion furnace by pre-deposition at 950°C and drive-in process at 1080°C . The initial emitter sheet resistance was $30\ \Omega/\text{sq}$. and then boron silicate glass (BSG) was removed by dipping in 20% Hydrogen Fluoride (HF) and 20% hydrochloric (HCl) acid for 1 min. The boron diffused emitter was etched back by the acid solution to give a high R_s of $70\text{--}80\ \Omega/\text{sq}$. The rear surface was formed by silicon oxide layer and poly-BSF

layer. The silicon oxide layer was grown by plasma enhanced chemical vapor deposition (PECVD) system. The RF power and substrate temperature were varied in the range of $25\text{--}400\ \text{W}$ and $200\text{--}400^\circ\text{C}$ whereas the N_2O gas of 50 sccm was fixed. First, the RF power was varied and then the temperature was varied. The best results were applied to the next experiment for optimization. The process pressure was set at 150 mTorr and the thickness of the silicon oxide layer was varied from 1.4 to 1.8 nm by controlling the process time. The thickness of the thin film was measured using an ellipsometry. In order to verify the passivation characteristics, a 20 nm thick phosphorus-doped a-Si layer was deposited on both sides of n-type Si wafer [7]. It was then annealed at 900°C in N_2 atmosphere to form a poly-BSF layer [8]. In addition, heat treatment with forming gas at 400°C was performed for 30 min 80 nm thick SiN_x with a refractive index, n , of 2.05 was deposited by PECVD on the front side for both passivation and antireflection coating (ARC) layer. The front electrode was formed using a mixture paste of silver and aluminum by screen printing. The rear electrode was formed by Ag/Al double layer using evaporation system. The lifetime and iV_{oc} were measured using a lifetime tester (Sinton WCT-120). The measured lifetime values were used to calculate SRV [6]. The change in SiO_x bond structure and the effect of passivation depending on the variable conditions were analyzed through XPS.

The optimized SiO_x layer was applied to n-type Si wafer based TOPCon cell to make solar cells. The fabricated cells were characterized by using illuminated current-voltage (LIV) measurements was performed by PASAN cell tester (model CT801) under the global spectrum of AM 1.5 condition. The conversion efficiencies and QE (Quantum Efficiency) were measured using an incident photon to current conversion efficiency (IPCE) measurement (QEX7) system.

3. Results and discussion

The surface passivation quality of the plasma grown oxide was

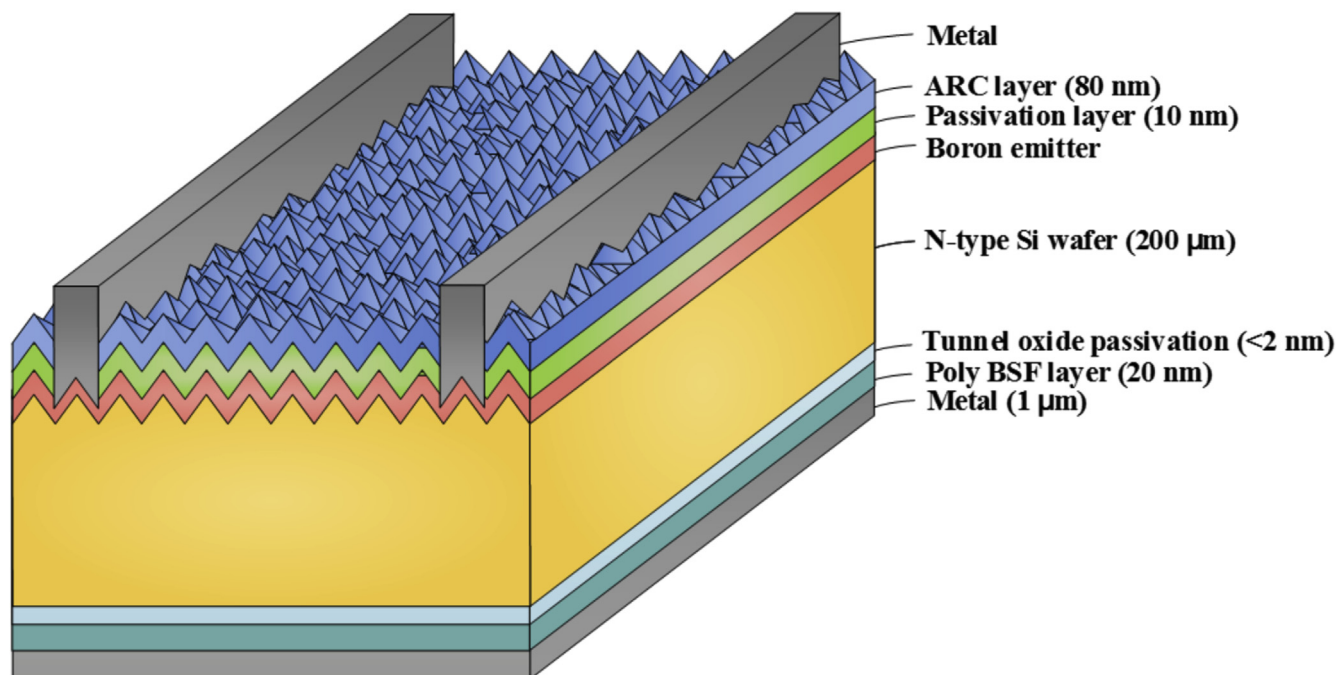


Fig. 1. Schematic of the solar cell structure used for this study.

tested on the symmetrical lifetime samples. The RF power was varied from 25 to 400 W in order to minimize the damage to the surface of the silicon wafer and to obtain excellent passivation effects. Surface Recombination Velocity (SRV) was calculated using the lifetime value using the following equation (2) [11].

$$\frac{1}{\tau_{eff}} = \frac{1}{\tau_{bulk}} + \frac{2S}{W} \quad (2)$$

where τ_{eff} is the effective lifetime, τ_{bulk} is the bulk lifetime and S is the surface recombination velocity. Fig. 2 (a) depicts the implied V_{oc} and SRV values achieved with the plasma grown oxides with RF power. iV_{oc} values increases from 715 mV to 730 mV and SRV reduces from 13 cm/s to 6 cm/s for the increase in RF power from 25 W to 200 W. Fig. 2 (b) shows SRV and iV_{oc} dependence on the substrate temperature. The graph shows that as the substrate temperature increases, the passivation effect increases.

From Fig. 3 (a), it can be seen that the D_{it} increases with increasing RF power. It shows that as the RF power is increased, the plasma damage on the silicon wafer surface is increased. In other words, RF power of more than 200 W increases the plasma damage on the wafer surface resulting in a reduction of the passivation effect [12]. However, at low RF power of less than 200 W, the radical of N_2O gas is not formed well, resulting in low deposition rate and passivation characteristics [13,14]. At 200 W, iV_{oc} of 733 mV showed

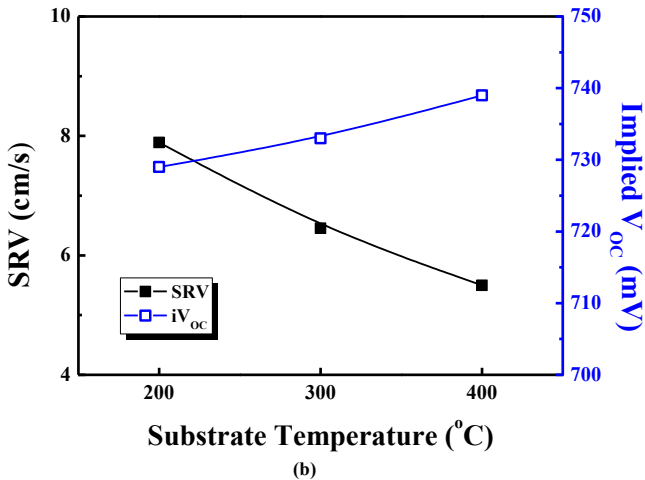
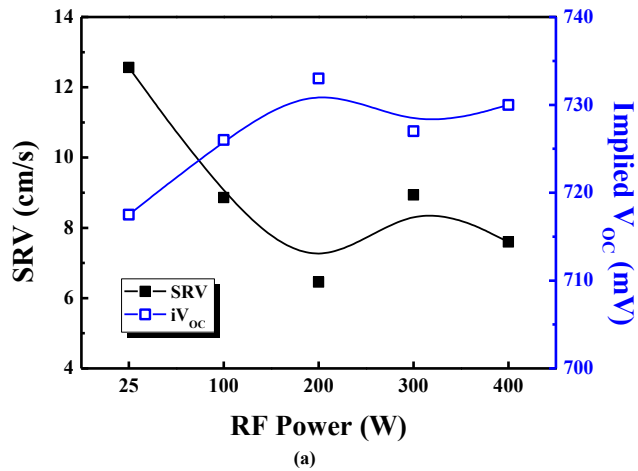


Fig. 2. SRV and iV_{oc} data (a) RF Power is varied, (b) Substrate Temperature is varied.

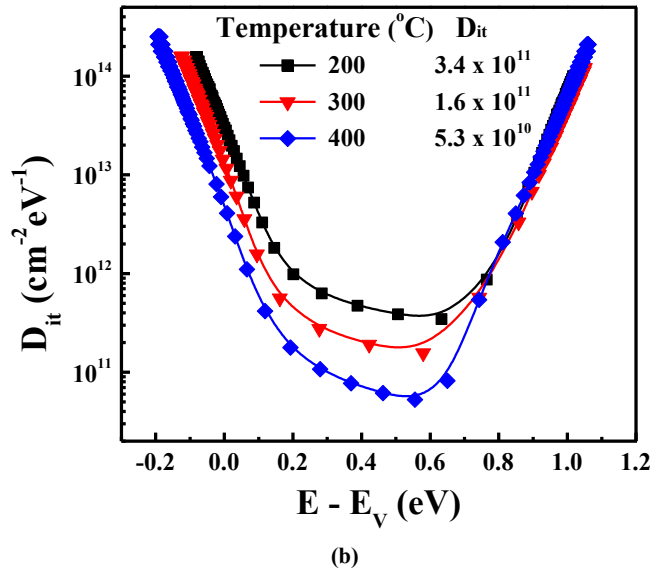
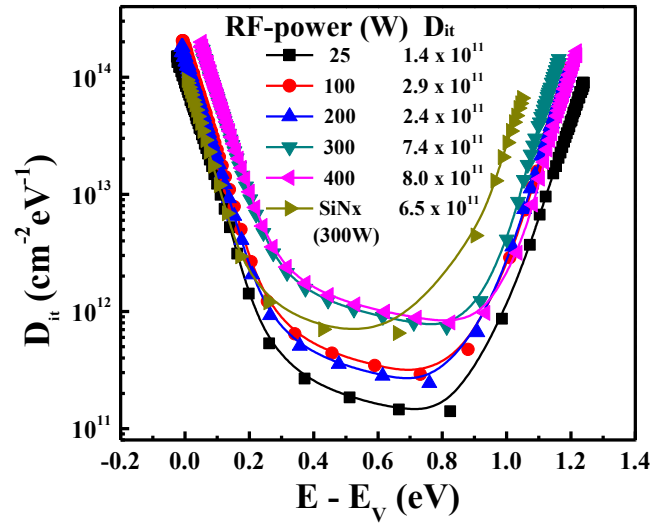


Fig. 3. The calculated interface state distribution D_{it} (a) RF Power is varied, (b) Substrate Temperature is varied.

the best passivation effect. The silicon oxide film growth experiment was carried varying the substrate temperature to 200, 300, and 400 °C with the fixed RF power of 200 W, a process pressure of 150 mTorr and N_2O gas of 50 sccm. Fig. 3 (b) shows that as the temperature increases, D_{it} , the defect at the interface decreases, resulting in the improved passivation. The SRV of 5.5 cm/s and iV_{oc} of 739 mV showed the best passivation effect at 400 °C.

Si (2p) bonds were analyzed by X-ray photoelectron spectroscopy (XPS) to determine the stoichiometry suboxide (Si^{1+} , Si^{2+}) formed in the silicon oxide layer grown at different substrate temperatures and its effect on the passivation. Fig. 4 (a) shows that as the temperature increases, the Si (2p) peak shifts to about 0.4 eV toward higher binding energy. Fig. 4 (b), (c) and (d) show $Si^+(100.6$ eV), $Si^{2+}(101.7$ eV), $Si^{3+}(102.6$ eV) and $Si^{4+}(103.4$ eV) peaks change as temperature increases. The peak of the stoichiometric SiO_2 appears at a binding energy of 103.4 eV [15]. In the case of the SiO_x layer, it is known that high quality passivation layer is

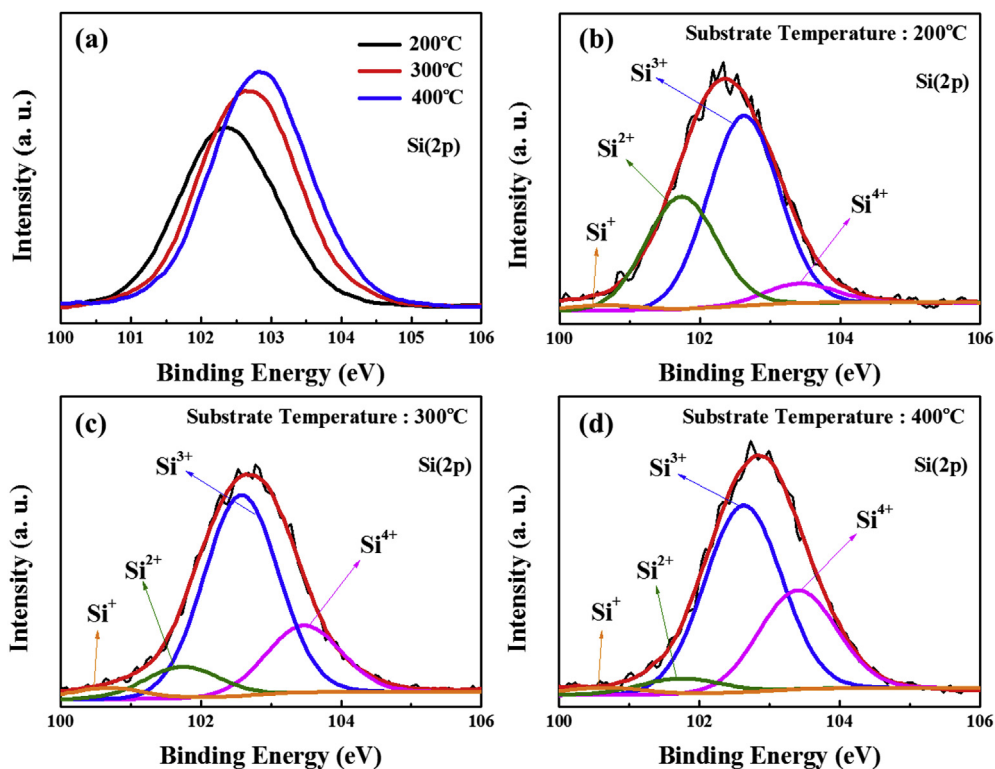


Fig. 4. (a) The Si(2p) XPS spectra of silicon oxide films on a Si(100) surface. (b), (c), (d) XPS peak analysis for comparison of Si²⁺ and Si⁴⁺ peak intensity. The films were deposited at different substrate temperatures.

obtained when the bond is formed with SiO₂. In the case of the silicon oxide film grown at 200 °C, many Si²⁺ (SiO₂) peak components appeared. For the silicon oxide layer grown at 400 °C with the best passivation characteristics, the Si²⁺ peak component decreased and Si⁴⁺ peak showed an increase as obtained by He et al. [16]. For the silicon oxide grown using N₂O gas plasma, it can be assumed that the higher the substrate temperature, the more stoichiometric SiO₂ bonds are formed. The silicon oxide film grown at the substrate temperature of 400 °C exhibited low SRV and high *i*V_{oc}.

The optimized oxide layer was applied to TOPCon cell to fabricate solar cells. Fig. 5 shows the cell characteristics dependence on the SRV. *J*_{sc} and *V*_{oc} increased as SRV decreased. The best cell showed *J*_{sc} of 41.04 mA/cm², *V*_{oc} of 644 mV, FF of 72.87% and Eff. of 19.25%. Though the plasma grown tunnel oxide provide excellent interface passivation, the tunnel oxide passivated rear contact should allow an efficient transport of majority carriers to enable high FF. However, the FF of 72.9% obtained is relatively low, compared with the reference cell of 76.2%. This is ascribed to the high series resistance and slight increase in ideality factor in our current tunnel oxide passivated devices.

Fig. 6 shows the results of light I-V measurement with different passivation layers on the n-type crystalline silicon solar cell. For the solar cell using tunnel oxide grown with N₂O plasma, *J*_{sc} and *V*_{oc} were improved by 0.2 mA/cm² and 11 mV, respectively, compared with the solar cell using tunnel oxide grown using the wet chemical. The results of the Suns-*V*_{oc} measurements show that the maximum *V*_{oc} is 661 mV under optimized conditions and the solar cell efficiency of 21.15% is obtained when *J*_{sc} is 40 mA/cm². In addition, if the efficiency is recalculated with the actually measured *J*_{sc} of 41 mA/cm², the light conversion efficiency up to 21.68% can be achieved.

When the tunnel oxide layer is applied to the rear passivation

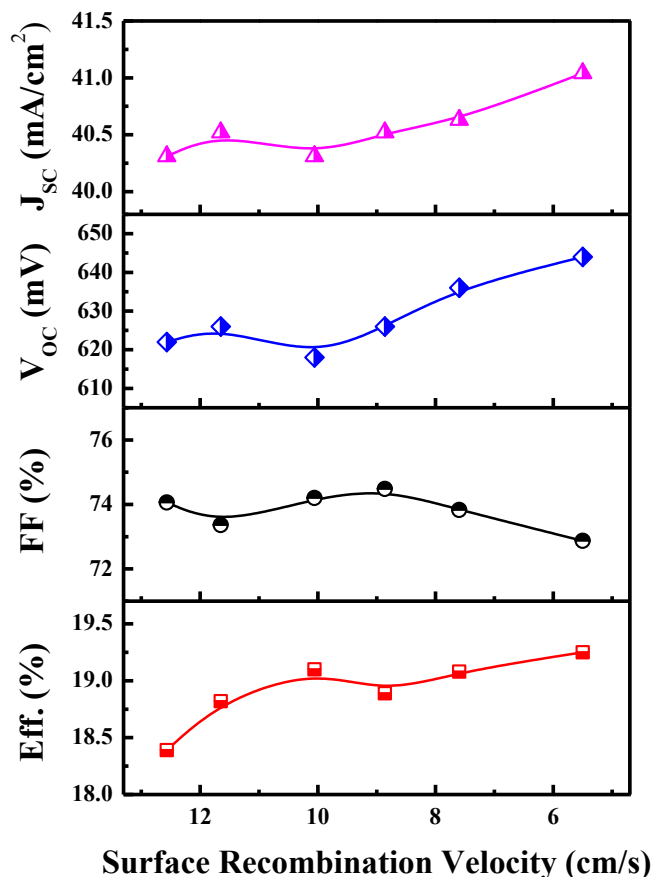


Fig. 5. The result of Light I-V measurement of different oxide conditions.

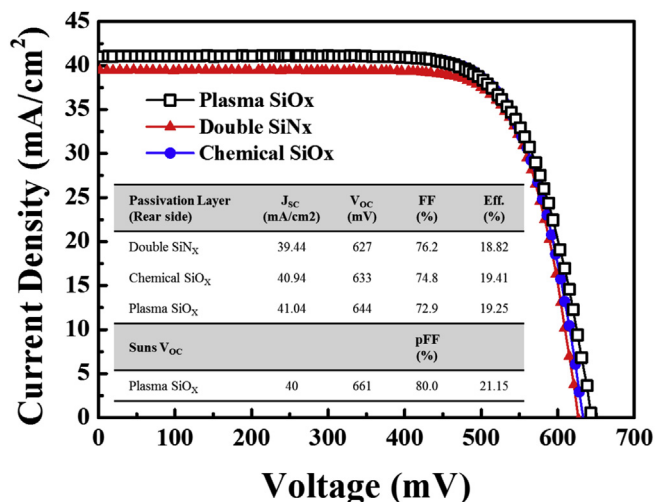


Fig. 6. Light I-V curve of solar cells with different rear side passivation structures.

layer of the n-type c-Si solar cell, the J_{sc} and V_{oc} are improved compared with the conventional SiN_x passivation. It is due to the tunneling effect of less than 2 nm thick tunnel oxide layer. The electrons pass through the oxide layer and collected by electrodes and holes are blocked. The carriers get separated and the recombination is reduced. This leads to an increase in the carrier collection rate and eventually an increase in current and voltage [17]. The quantum efficiency of the incident light was measured by quantum efficiency (QE) measurement. As shown in Fig. 7, higher quantum efficiency can be confirmed compared with the SiN_x passivation cell in a long wavelength of over 800 nm. In the long wavelength region, the main recombination occurs at the rear side. The recombination of electrons and holes is reduced due to the passivation effect of SiO_x applied to the rear side. Also, since the back electrode serves as a reflector, the efficiency of the electron-hole generation is increased due to the reflection of the incident light at the long wavelength. Better solar cell characteristic such as J_{sc} and V_{oc} are obtained for the solar cell with the N₂O plasma SiO_x layer compared to the one with the chemical SiO_x layer.

4. Conclusion

The best passivation effect, low SRV of 5.5 cm/s and iV_{oc} of 739 mV were obtained with the RF power of 200 W and temperature of 400 °C. Through the XPS analysis, it was confirmed that the passivation effects were improved with the Si⁴⁺ peak (SiO₂ bonding) component, and the SiO₂ bond structure increased with increasing substrate temperature. It was confirmed by XPS peak analysis that the most bonding components were present at 400 °C. The optimized SiO_x film had low D_{it} characteristics of $5.3 \times 10^{10} \text{ cm}^{-2} \text{ eV}^{-1}$. This silicon oxide film was applied to actual solar cell fabrication and it was compared to the cell with the chemically grown tunnel oxide layer. J_{sc} and V_{oc} increased by 0.2 mA/cm² and 11 mV, respectively. Suns- V_{oc} measurement results showed V_{oc} of 661 mV, J_{sc} of 40 mA/cm², pFF of 80.0% and eff. 21.15%. In this study, we have investigated the efficiency improvement by improving the backside passivation layer of the n-type crystalline silicon solar cell by applying SiO_x layer using N₂O plasma

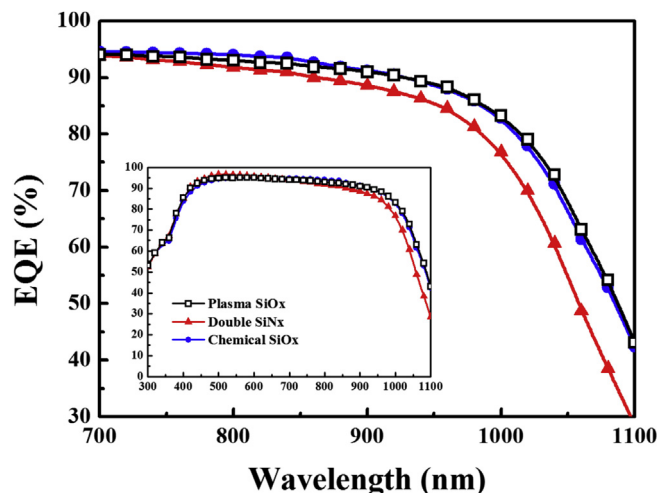


Fig. 7. The external quantum efficiency (EQE) of the solar cells with different rear side passivation structures.

growth and poly-BSF layer. It is expected that a solar cell with higher efficiency can be fabricated using the improved passivation properties.

Acknowledgment

This work was supported by the New & Renewable Energy Core Technology Program of the Korea Institute of Energy Technology Evaluation and Planning (KETEP), granted financial resource from the Ministry of Trade, Industry & Energy, Republic of Korea. (No: 20163010012230).

References

- [1] Graham Fisher, Michael R. Seacrist, Robert W. Standley, in Proc. of IEEE, 100, 1454–1474 (2012).
- [2] ITRPV, Int. Technol. Roadmap Photovoltaic. 7 (2016).
- [3] Hemant Kumar, R. Soc. Chem. 4 (2013) 3779–3804.
- [4] Nagarajan Balaji, Cheolmin Park, Yongwoo Lee, Sungwook Jung, Junsin Yi, Vacuum 96 (October 2013) 69–72.
- [5] Gyuhoo Choi, Nagarajan Balaji, Cheolmin Park, Jaewoo Choi, Seunghwan Lee, Jungmo Kim, Minkyu Ju, Youn-Jung Lee, Junsin Yi, Vacuum 101 (March 2014) 22–26.
- [6] W.C. Lee, C. Hu, IEEE Trans. Electron Devices 48 (7) (2001) 1366–1373.
- [7] Frank Feldmann, Martin Bivour, Christian Reichel, Martin Hermle, Stefan W. Glunz, Sol. Energy Mater. Sol. Cells 120 (2014) 270–274.
- [8] Anamaria Moldovan, Frank Feldmann, Martin Zimmer, Jochen Rentsch, Jan Benick, Martin Hermle, Sol. Energy Mater. Sol. Cells 142 (2015) 123–127.
- [9] Frank Feldmann, Martin Bivour, Christian Reichel, Martin Hermle, Stefan W. Glunz, Sol. Energy Mater. Sol. Cells 131 (2014) 100–104.
- [10] H.K. Asuha, O. Maida, M. Takahashi, H. Iwasa, Nitric acid oxidation of Si to form ultrathin silicon dioxide layers with a low leakage current density, J. Appl. Phys. 94 (2003) 7328–7335.
- [11] Jed Brody, Ajeet Rohatgi, Alan Ristow, Sol. Energy Mater. Sol. Cells 77 (2003) 293–301.
- [12] H.P. Zhou, S. Xu, S.Q. Xiao, “High-Density Plasma-enhanced Chemical Vapor Deposition of Si-based Materials for Solar Cell Applications”-chemical Vapor Deposition, 2016.
- [13] Y.T. Kim, S.M. Cho, Y.G. Seo, H.D. Yoon, Y.M. Im, D.H. Yoon, Cryst. Res. Technol. 37 (2002) 1257–1263.
- [14] Mark J. Kushner, J. Appl. Phys. 74 (1993) 6538.
- [15] Anamaria Moldovan, Energy Procedia 55 (2014) 834–844.
- [16] J.W. He, X. Xu, J.S. Corneille, D.W. Goodman, Surf. Sci. 279 (1) (1992) 119–126.
- [17] F. Feldmann, M. Simon, M. Bivour, C. Reichel, M. Hermle, S.W. Glunz, Appl. Phys. Lett. 104 (2014) 181105.